Journal of Catalysis **193,** 207–223 (2000)
doi:10.1006/jcat.2000.2881, available online at http://www.idealibrary.com on IDEAL®

Role of Hydrogen Spillover in Methanol Synthesis over Cu/ZrO_2

Kwang-Deog Jung and Alexis T. Bell[1]

Chemical Sciences Division, Lawrence Berkeley National Laboratory, Berkeley, California 94720; and Department of Chemical Engineering, University of California, Berkeley, California 94720-1462

Received September 27, 1999; revised March 27, 2000; accepted March 28, 2000

Recent studies have shown that the synthesis of methanol from both CO and CO_2 over Cu/ZrO_2 involves the spillover of H atoms formed on Cu to the surface of ZrO_2. The atomic H then participates in the hydrogenation of carbon-containing species (i.e., HCOO–Zr and HCO_3–Zr) to methanol. The present study examines the dynamics of H/D exchange of HO–Zr, HCOO–Zr, and CH_3O–Zr groups present on the surface of ZrO_2 and Cu/ZrO_2 by means of *in situ* infrared spectroscopy. The rate of H/D exchange of HO–Zr groups is much more rapid in the presence than in the absence of Cu dispersed on the surface of ZrO_2. This effect is attributed to the higher effectiveness of Cu to dissociate $H_2(D_2)$. While adsorbed water significantly inhibits the rate of H/D exchange on ZrO_2, the opposite effect is observed for Cu/ZrO_2. The reason is that adsorbed water inhibits the dissociation of $H_2(D_2)$ on the surface of ZrO_2 but not on the surface of Cu. Adsorbed water facilitates the transport of H(D) atoms formed on the surface of Cu across the surface of ZrO_2 as a consequence of hydrogen bonding between adsorbed H_2O and HO–Zr groups. Formate groups are formed on the surface of ZrO_2 primarily via the process $CO_{(g)} + HO\text{–}Zr \rightarrow HCOO\text{–}Zr$. Formate groups can also form on the surface of Cu and spill over onto the surface of ZrO_2. The presence of formate groups inhibits the rate of H/D exchange of HO–Zr groups. H/D exchange of HCOO–Zr is also observed but occurs at a slower rate than the isotopic exchange of HO–Zr groups. As in the absence of formate groups, adsorbed water inhibits the rate of H/D exchange for ZrO_2 but enhances it for Cu/ZrO_2. The dynamics of H/D exchange are compared with the dynamics of methanol formation as measured by the rate of CH_3O–Zr formation on Cu/ZrO_2. On the basis of this analysis it is concluded that the rate of hydrogen spillover from Cu is more than an order of magnitude faster than the rate of methanol formation, and, hence, not a rate-limiting step in the synthesis of methanol over Cu/ZrO_2.

Key Words: **hydrogen spill over; methanol synthesis; Cu/ZrO_2.**

INTRODUCTION

Zirconia-supported copper exhibits high activity for the synthesis of methanol from either CO/H_2 or CO_2/H_2 (1–18). Recent studies of the mechanism of methanol synthesis and decomposition over zirconia-containing copper catalysts have revealed that the zirconia is an active component of the catalyst (14–18). In the case of CO_2 hydrogenation, CO_2 adsorbs on the zirconia to form bicarbonates species, which undergo hydrogenation to produce formate, methylenebisoxy, and finally methoxide species (17). The hydrogen required for the progressive hydrogenation of the zirconia-bound carbonaceous species is provided by spillover of H atoms produced by the dissociative adsorption of H_2 on Cu. Conversion of CO_2 to CO via the reverse water–gas shift reaction also occurs on the surface of Cu. In the case of CO hydrogenation, CO adsorbs on the zirconia to form formate species, which then undergo sequential hydrogenation to form methoxy species (18). Methoxy species derived from either CO or CO_2 hydrogenation are converted to methanol either by reductive elimination or by hydrolysis. The first of these processes is slow and is the dominant pathway to methanol produced by CO hydrogenation, whereas the latter process is significantly more rapid and is the primary pathway to methanol produced by CO_2 hydrogenation.

The importance of hydrogen spillover in the synthesis of methanol from CO and CO_2 over zirconia-containing Cu catalysts engenders an interest in understanding the dynamics of hydrogen transport on the surface of zirconia and the role of Cu in this process. Studies of H–D exchange on monoclinic zirconia suggest that molecular hydrogen (or deuterium) dissociates either heterolytically or homolytically and then diffuses rapidly across the oxide surface (19). The rate of isotopic exchange between atomically adsorbed D atoms and OH groups on the surface of zirconia is proportional to the fractional coverage of the oxide by OH groups and is half order in the partial pressure of D_2. The apparent activation energies for the H/D exchange of terminal and bridging OH groups are 35 kJ/mol and 41 kJ/mol, respectively. When formate species are produced on the surface of zirconia, exchange of HCOO with D_2 occurs via an activated process characterized by an apparent activation energy of 95 kJ/mol; however, no H/D exchange is observed between OD and HCOO groups (20). By contrast, methoxy species exchange H atoms in the methyl group with surface OD groups, even in the absence of gaseous D_2. The activation energy measured for H/D exchange in methoxy groups

[1] To whom correspondence should be addressed. E-mail: Bell@cchem.berkeley.edu.

0021-9517/00 $35.00

is 127 kJ/mol. Studies conducted with Rh dispersed on the surface of monoclinic ZrO_2 indicate that the rate of isotopic exchange of D with surface OH groups is significantly higher than that in the absence of Rh (21), and it is hypothesized that the rate of isotopic exchange is rate-limited by diffusive transport across the surface of ZrO_2.

The present study was undertaken to determine the effects of various parameters on the rates of hydrogen migration and the rates of H/D exchange for various species adsorbed on the surface of ZrO_2. *In situ* infrared spectroscopy was used to observe the dynamics of isotopic exchange. Particular attention was given to determining the influence of dispersed Cu on rates of H(D) atom generation and the dynamics of H/D exchange, as well as the effects of $H_2(D_2)$ partial pressure and temperature on the rates of these processes. The influence of adsorbed water was also investigated. An ultimate objective of the present investigation was to establish whether the dynamics of hydrogen spillover on zirconia are rate-limiting in the synthesis of methanol.

EXPERIMENTAL

The preparation and characterization of the Cu/ZrO_2, ZrO_2, and $Cu/ZrO_2/SiO_2$ catalysts used in this study have been described elsewhere (10, 17, 18). The Cu and Zr contents of the catalysts were determined by X-ray fluorescence and the Cu surface areas of the catalysts were determined by N_2O titration (10). These methods showed that the Cu/ZrO_2 catalyst contained 5.7 wt% Cu with a specific Cu surface area of 1.68 m^2/g (4.5% Cu dispersion); the $Cu/ZrO_2/SiO_2$ catalyst contained 5.7 wt% Cu and 16.4 wt% ZrO_2 with a Cu surface area of 1.24 m^2/g (3.3% Cu dispersion). The BET surface area of the ZrO_2 was determined to be 20 m^2/g. XRD and the infrared spectrum of hydroxyl groups on the support surface indicate that the support is comprised predominantly of monoclinic ZrO_2.

Matheson UHP H_2, D_2, He, CO, and Coleman instrument purity CO_2 were purified prior to use. Hydrogen and deuterium were passed through a Deoxo unit (Engelhard) to remove O_2 impurities by forming water which was subsequently removed by a molecular sieve trap. He gas was passed through an oxysorb (CrO_2) trap to remove O_2 and then a molecular sieve trap. CO was passed through a bed of glass beads maintained at 573 K to decompose iron carbonyls, followed by passage through an ascarite trap to remove CO_2 and a molecular sieve trap (3A Davidson grade 564) to remove water. CO_2 was passed through a hopcalite trap (80% MnO_2 + 20% CuO) to remove CO and a molecular sieve trap to remove water. Purified gases were delivered to the infrared cell via Tylan Model FC-280 mass flow controllers.

In situ transmission infrared spectroscopy was performed using 2-cm-diameter catalyst disks, weighing approximately 55 mg. The catalyst disks were contained in a low-dead-volume infrared cell (22). Infrared spectra were collected using a Nicolet Magna 750 series II FTIR spectrometer. Signals were obtained from a narrow-band MCT detector. *In situ* absorbance spectra were obtained by collecting 21–64 scans at 4 cm^{-1} resolution. Each spectrum was then referenced to a spectrum of the catalyst collected at the same temperature under He or H_2 flow, as appropriate. Electrical resistance heaters were used to heat the cell. An Omega Series CN-2010 programmable temperature controller controlled the cell temperature.

Prior to each experiment with a fresh sample, the catalyst was reduced in 10% H_2/He flowing at 60 cm^3/min. The reduction temperature was raised to 2 K/min from ambient to 523 K, after which the catalyst was further reduced at 523 K for >8 h in pure H_2 flowing at 60 ml/min. Subsequent reductions were all performed at 523 K, but varied in time (always >8 h) to ensure that observable surface species had been removed.

RESULTS

Dynamics of CO_2 Hydrogenation

Figure 1 shows spectra obtained during CO_2 hydrogenation over Cu/ZrO_2 at 523 K and a total pressure of 650 kPa. The feed is switched from He to H_2/CO_2 (3/1) flowing at a total flow rate of 60 cm^3/min. Strong peaks are observed at 2966, 2873, 1570, 1385, and 1372 cm^{-1} for bidentate formate on ZrO_2 (b-HCOO–Zr) (23–25), and at 2927 and 2821 cm^{-1} for methoxy on ZrO_2 (CH_3O–Zr) (14, 24). A broad band of low intensity is seen between 1475 cm^{-1} and 1440 cm^{-1}. Within this region, bands have been observed at 1473 cm^{-1} for monodentate carbonate (m-CO_3–Zr) (17, 26), at 1457 cm^{-1} for bidentate bicarbonate on ZrO_2 (b-HCO_3–Zr) (17, 23), and at 1445 cm^{-1} for ionic carbonate (i-CO_3^{2-}) (17, 26). The weak feature at 1311 cm^{-1} is most likely due to bidentate carbonate on ZrO_2 (b-CO_3^{2-}–Zr) (23, 27, 28).

Figure 2 shows spectra obtained on ZrO_2 under the same condition as those given for Fig. 1. Features are observed at 2965, 2881, 1550–1568, 1385, and 1370 cm^{-1} for bidentate formate (b-HCOO–Zr) and 2931 and 2827 cm^{-1} for methoxy (CH_3O–Zr). Features for bidentate bicarbonate are observable at 1610 and 1452–1462 cm^{-1} (b-HCO_3) (27–29). The band peak at 1589 cm^{-1} is identical to that assigned to monodentate bicarbonate species on Cu/SiO_2 (m-HCOO–Cu) (30, 31), and consequently, the peak at 1589 cm^{-1} is assigned by analogy to m-HCOO–Zr.

A few minutes after the reaction starts, a peak for ionic carbonate is observed at 1421 cm^{-1} (26). During reaction, the intensities of the bands for both b-HCOO–Zr and CH_3O–Zr increase, while those for carbonates decrease, suggesting that methoxy species are formed by serial hydrogenation of formate species derived from carbonate species. It is interesting to note that the frequencies associated with

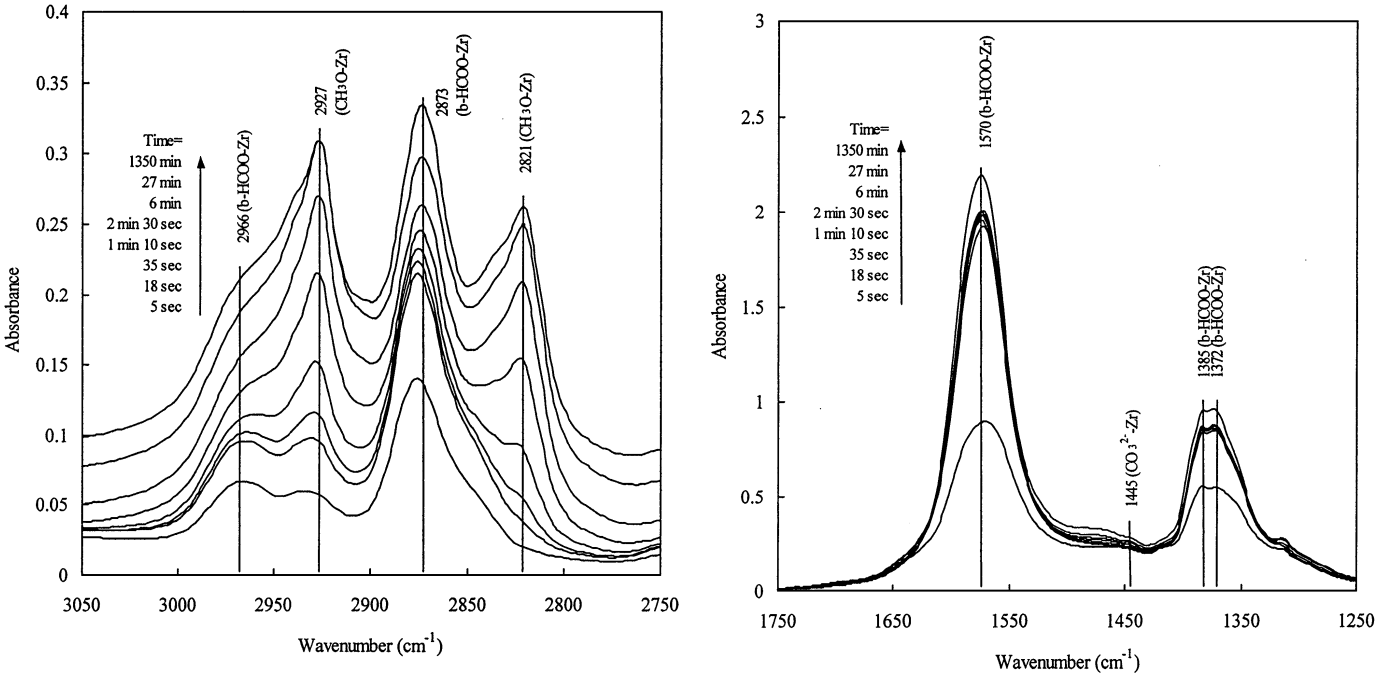

FIG. 1. Infrared spectra taken during exposure of Cu/ZrO_2 at 523 K to 488 kPa H_2 and 162 kPa CO_2 flowing at a total rate of 60 cm^3/min. All spectra are referenced to Cu/ZrO_2 reduced in flowing H_2 at 650 kPa H_2 at 523 K.

formate and bicarbonate species (2965–2966, 1568–1570, 1385, 1370–1372 cm^{-1}) are the same on both Cu/ZrO_2 and ZrO_2, whereas the frequencies associated with C–H stretching vibrations in methoxy groups are 4–6 cm^{-1} lower for Cu/ZrO_2 (2927, 2821 cm^{-1}) than those for ZrO_2 (2931, 2827 cm^{-1}).

Figure 3 shows the normalized intensities of b-HCOO–Zr and CH_3O–Zr as a function of time when these species are

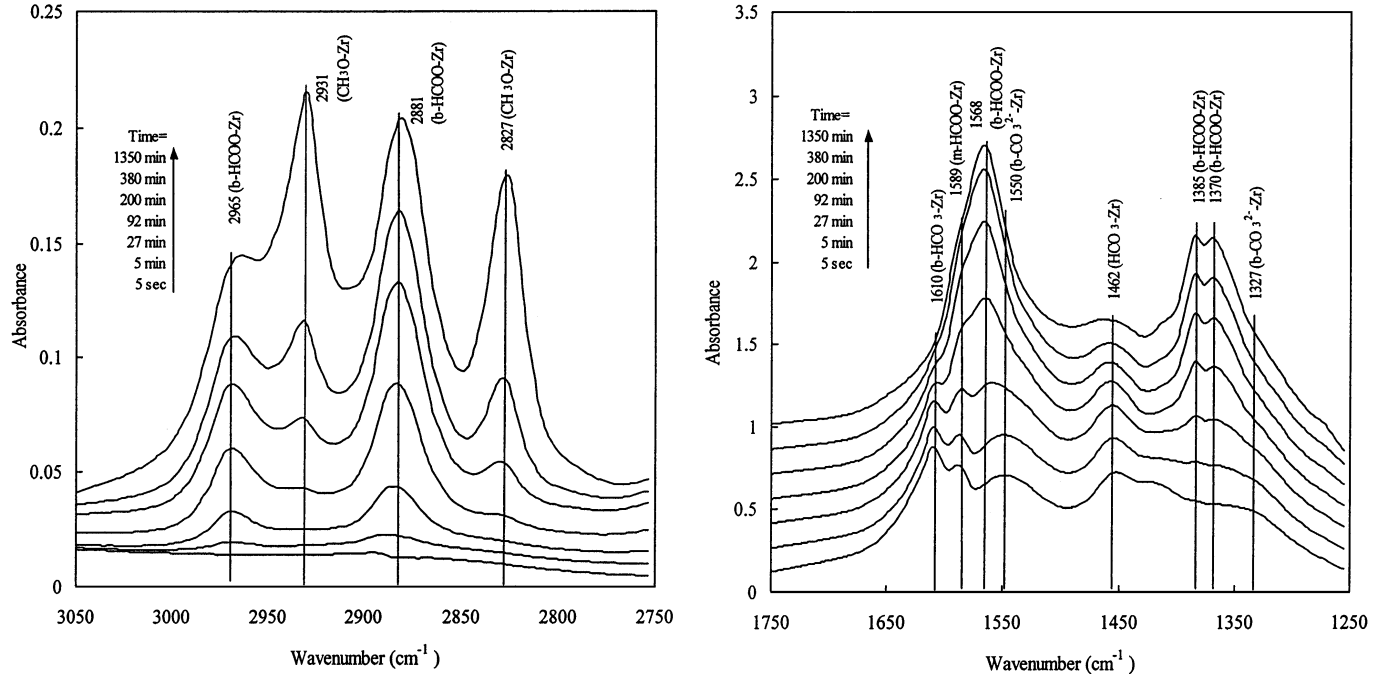

FIG. 2. Infrared spectra taken during exposure of ZrO_2 at 523 K to 488 kPa H_2 and 162 kPa CO_2 flowing at a total rate of 60 cm^3/min. All spectra are referenced to Cu/ZrO_2 reduced in flowing H_2 at 650 kPa H_2 at 523 K.

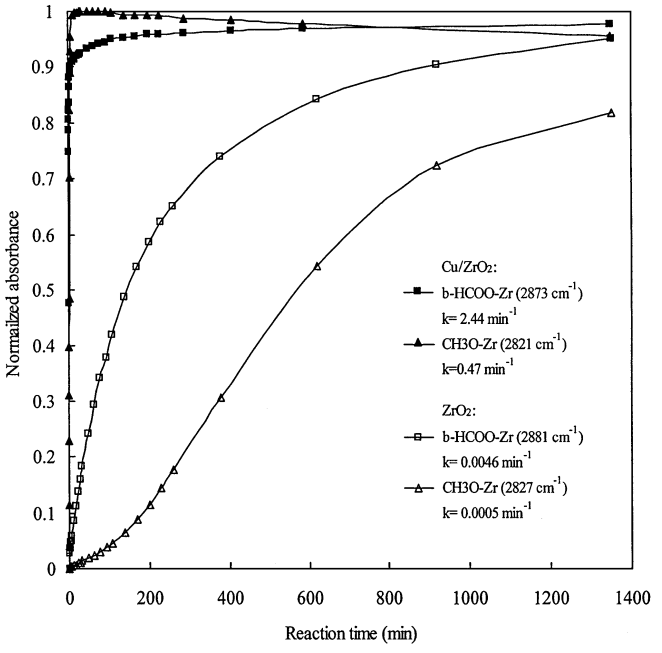

FIG. 3. Intensities of b-HCOO–Zr and CH_3O–Zr bands for both Cu/ZrO_2 and ZrO_2 taken from Figs. 1 and 2. Intensities are normalized to those observed at the end of the transient.

produced over ZrO_2 and Cu/ZrO_2. In each case, the peak intensities observed at the end of the transient shown (see Figs. 1 and 2) is used for normalization. It is noted that in the case of species such as CH_3O–Zr on ZrO_2 the response approaches unity at times much longer than those shown in Fig. 3. For ZrO_2 the normalized intensity of b-HCOO–Zr rises monotonically and reaches a value of 0.95 only after 1350 min. The transient for CH_3O–Zr species is significantly slower and exhibits a sigmoid character, suggesting that the CH_3O–Zr is produced as a secondary product by hydrogenation of b-HCOO–Zr (17). When Cu is present on the surface of ZrO_2, the transients for b-HCOO–Zr and CH_3O–Zr are more than 2 orders of magnitude faster than those observed in the absence of Cu. These observations strongly suggest that Cu enhances the rates of formation of b-HCOO–Zr and CH_3O–Zr by providing an efficient source atomic hydrogen of the carbonaceous species present on the surface of ZrO_2. Pseudo-first-order rate coefficients for the rates of HCOO–Zr and CH_3O–Zr formation on Cu/ZrO_2 and ZrO_2 are listed in the legend of Fig. 3. In calculating these rate coefficients it was assumed that the concentrations of all species except that being observed are constant.

H/D Exchange of Hydroxyl Groups

Figure 4 shows spectra obtained after switching from 650 kPa He to 488 kPa D_2 and 163 kPa He at 398 K flowing at a total flow rate of 60 cm^3/min. On both Cu/ZrO_2 and ZrO_2 (Fig. 4), O–H stretching vibrations are observed at 3758 cm^{-1} for terminal hydroxyl (t-OH) groups (26, 32) and at 3678 cm^{-1} (27, 29, 33) for bridged hydroxyl groups (b-OH). As soon as the catalysts are exposed to D_2, two

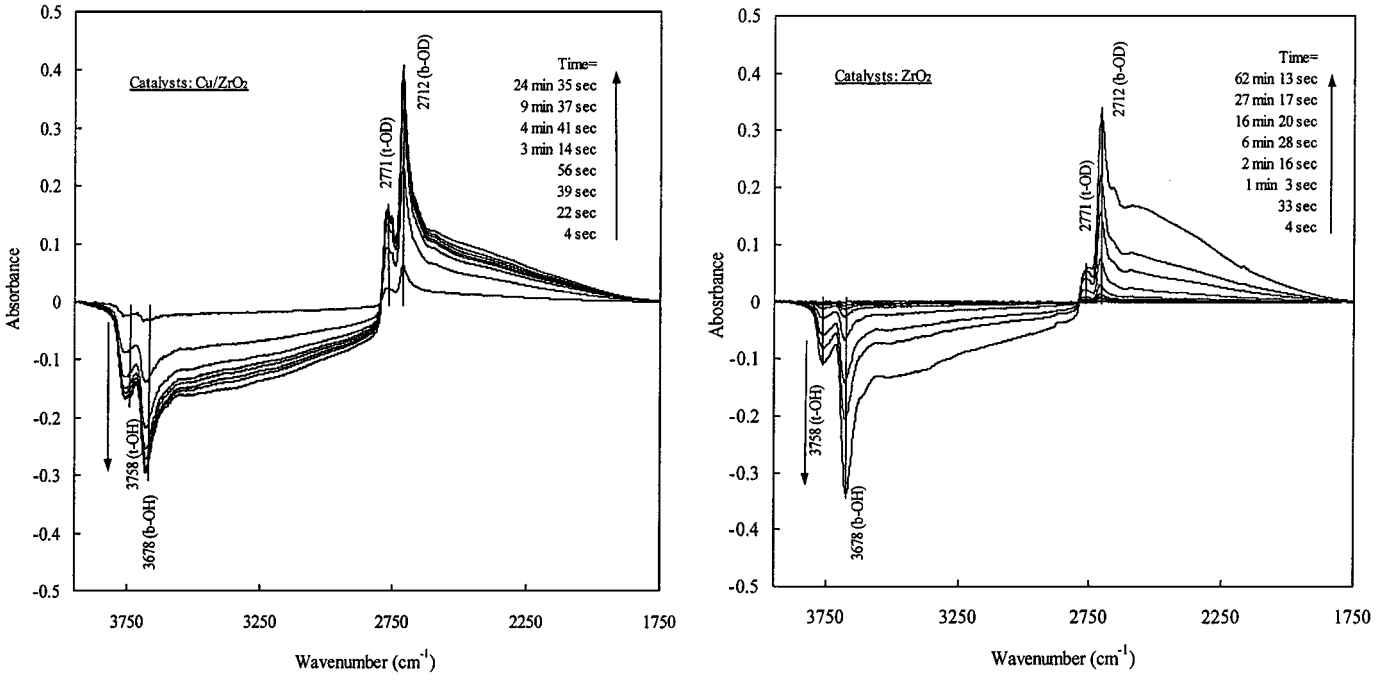

FIG. 4. Infrared spectra taken during exposure of both Cu/ZrO_2 and ZrO_2 at 398 K to 488 kPa D_2 and 162 kPa He flowing at a total flow of 60 ml/min. Spectra are referenced to Cu/ZrO_2 and ZrO_2 purged at 398 K in He flowing He at 650 kPa.

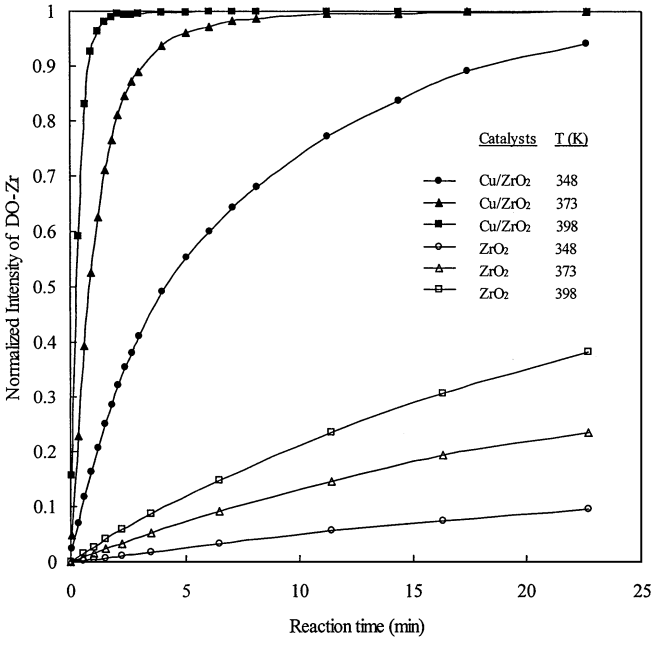

FIG. 5. Intensity of DO–Zr bands during exposure of both Cu/ZrO_2 and ZrO_2 at 348 K, 373 K, and 398 K to 488 kPa D_2 and 162 kPa He flowing at a total rate of 60 cm^3/min. Intensities are normalized to that for O–D stretching after all OH groups are exchanged for OD groups.

new peaks appear at 2712 and 2771 cm^{-1}, which can be assigned to terminal hydroxyl (t-OD) and bridged hydroxyl (b-OD), respectively.

Figure 5 shows the rate of H/D exchange of bridged hydroxyl groups at 348, 378, and 398 K on both Cu/ZrO_2 and ZrO_2. It is evident that the rate of exchange increases with temperature and is much higher for Cu/ZrO_2 than for ZrO_2. Table 1 shows apparent activation energies obtained from an Arrhenius plot. The apparent activation energies are 50 kJ/mol for Cu/ZrO_2 and 53 kJ/mol for ZrO_2. Also listed in Table 1 is the dependence of the rate of hydroxyl group H/D exchange determined at 398 K. The partial orders in deuterium are 0.25 for Cu/ZrO_2 and 0.74 for ZrO_2.

To investigate the effect of adsorbed water on the rate of H/D exchange of hydroxyl groups, the catalyst was purged in He at 523 K for at least 1 h following H_2 reduction, cooled to 323 K, and then exposed to H_2 saturated with H_2O ($P_{H_2O} = 3.2$ kPa) at 323 K for 10 min. Finally, the catalyst temperature was raised to the desired reaction temperature at the rate of 5 K/min. During this phase of the experiment and during the subsequent exposure of the catalyst to D_2, the supply of H_2O was discontinued. Figure 6 shows the normalized intensity of the OD band with the reaction time for Cu/ZrO_2 (at 373 K) and ZrO_2 (at 423 K). The reaction rate is slightly enhanced by the presence of adsorbed H_2O for Cu/ZrO_2, but is significantly suppressed for ZrO_2.

TABLE 1

Apparent Activation Energies and H_2 (D_2) Partial Pressure Dependence for the H/D Exchange of HO–Zr Groups on the Surface of ZrO_2 and Cu/ZrO_2

Catalyst	E_a (kJ/mol)	Partial order in D_2
ZrO_2 (without formate)	53	0.74
ZrO_2 (with formate)	66	1.24
Cu/ZrO_2 (without formate)	50	0.25
Cu/ZrO_2 (with formate)	72	0.54

H/D Exchange in the Presence of Formate Species

To investigate the effects of formate species on the dynamics of H/D exchange on the surface of zirconia, the catalyst was exposed to CO/He (1/3) mixture, after it had been purged at 523 K and 101 kPa for 1 h with He to remove any adsorbed hydrogen. As seen in Figs. 7 and 8, features are observed for b-HCOO–Zr at 2968, 2888, 1568, 1388, and 1371 cm^{-1} on Cu/ZrO_2 and at 2970, 2882, 1568, 1386, and 1370 cm^{-1} on ZrO_2. Terminal Zr–OH groups are observed at 3755 cm^{-1} on Cu/ZrO_2 and at 3733 cm^{-1} on ZrO_2. Bridged Zr–OH groups are observable at 3650 cm^{-1} on both Cu/ZrO_2 and ZrO_2. Traces of CH_3O–Zr are evident at 2836 and 2936 cm^{-1} on both Cu/ZrO_2 and ZrO_2. For both catalysts, the concentrations of terminal and bridged hydroxyl groups decrease during the reaction with CO to produce b-HCOO–Zr. After a few minutes, weak bands characteristic of CH_3O–Zr start to appear. One possibility for the appearance of CH_3O–Zr is that b-HCOO–Zr is hydrogenated by latent hydrogen, which is

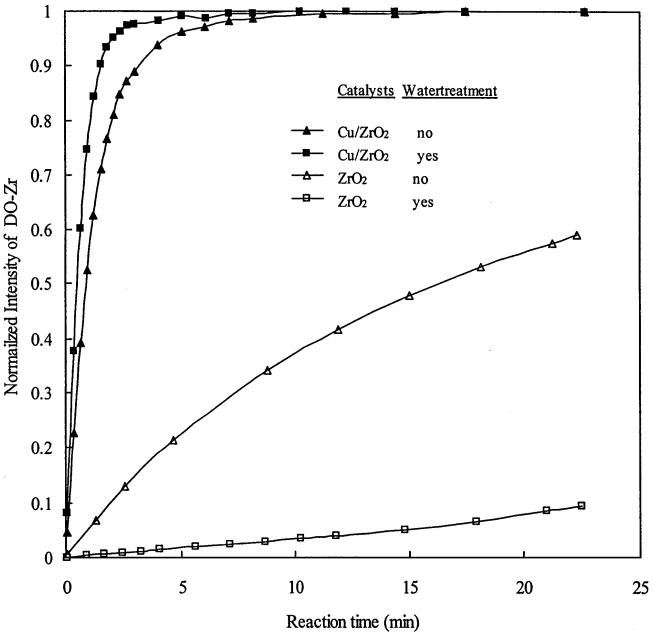

FIG. 6. Intensity of DO–Zr band during exposure of Cu/ZrO_2 and ZrO_2 at 423 K to 488 kPa D_2 and 162 kPa He flowing at a total rate of 60 cm^3/min after water treatment at 323 K. Intensities are normalized to that of DO–Zr after total H/D exchange.

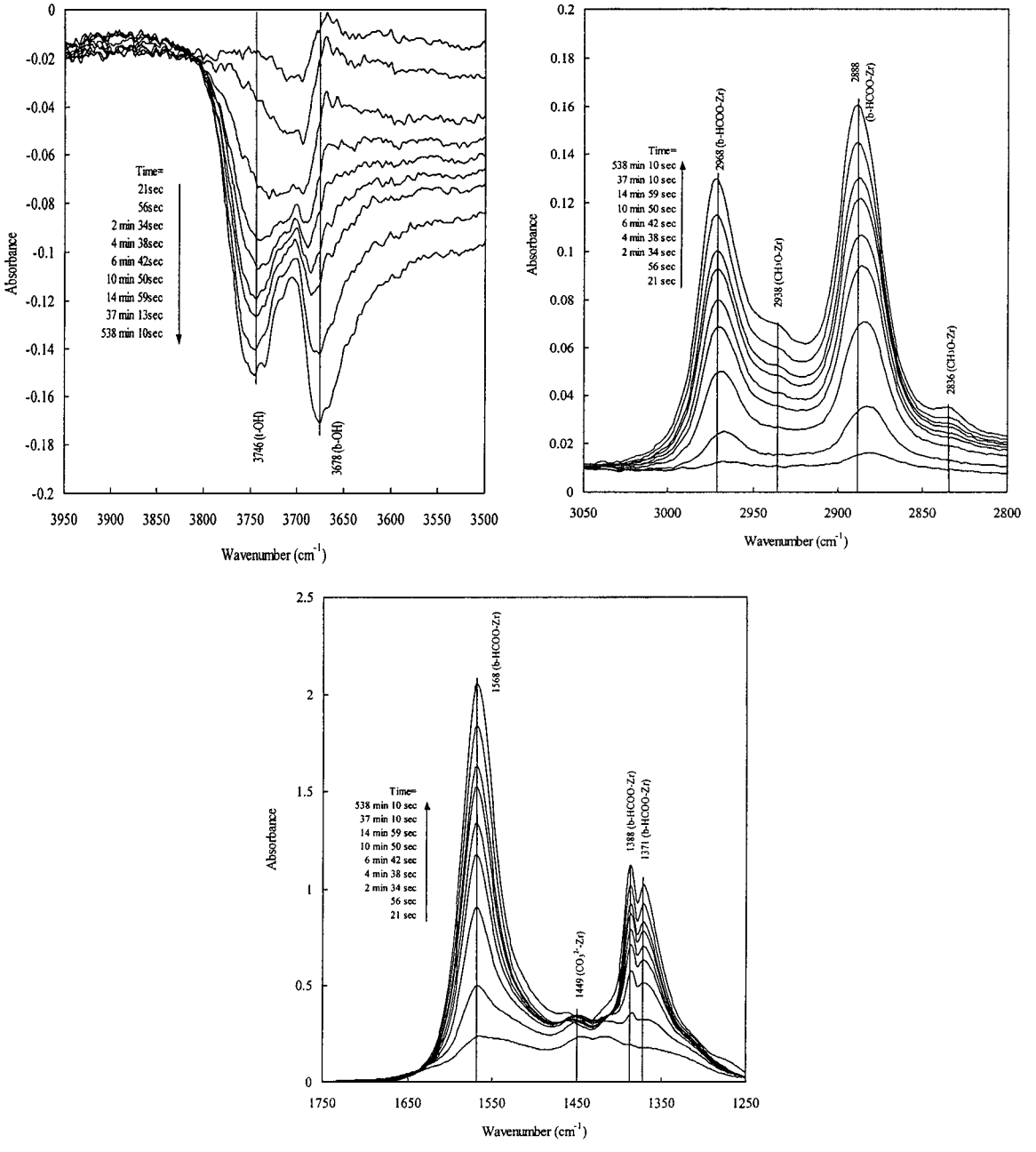

FIG. 7. Infrared spectra taken during exposure of Cu/ZrO_2 at 523 K to 488 kPa He and 162 kPa CO flowing at a total rate of 60 ml/min. Spectra are referenced to Cu/ZrO_2 under 650 kPa He flow at 523 K.

not removed during the He purge. On ZrO_2, the peak at 1568 cm^{-1} for C=O stretching is separated into two peaks at 1589 and 1556 cm^{-1}. The peak at 1568 cm^{-1}, assigned to m-HCOO–Zr, seems to be formed by repulsion among b-HCOO–Zr at high concentration.

Figure 9 shows the changes as a function of time in the normalized intensities of the bands associated with hydroxyl and formate species observed over Cu/ZrO_2 and ZrO_2 during CO adsorption. The intensities of the hydroxyl bands are normalized to the maximum intensities observed prior to reaction (see Figs. 7 and 8) and the intensity of the formate band is normalized to its maximum intensity after reaction. On Cu/ZrO_2, 78 and 62% of available terminal and bridging hydroxyls, respectively, are consumed to form formate groups up to the reaction time of 538 min. On ZrO_2, all terminal hydroxyl groups are reacted with CO to form formate, while 38% of bridged hydroxyls are consumed.

The effects of formate groups on the dynamics of H/D exchange of hydroxyl groups on the surface of Cu/ZrO_2 are presented in Fig. 10. Prior to initiation of H/D exchange,

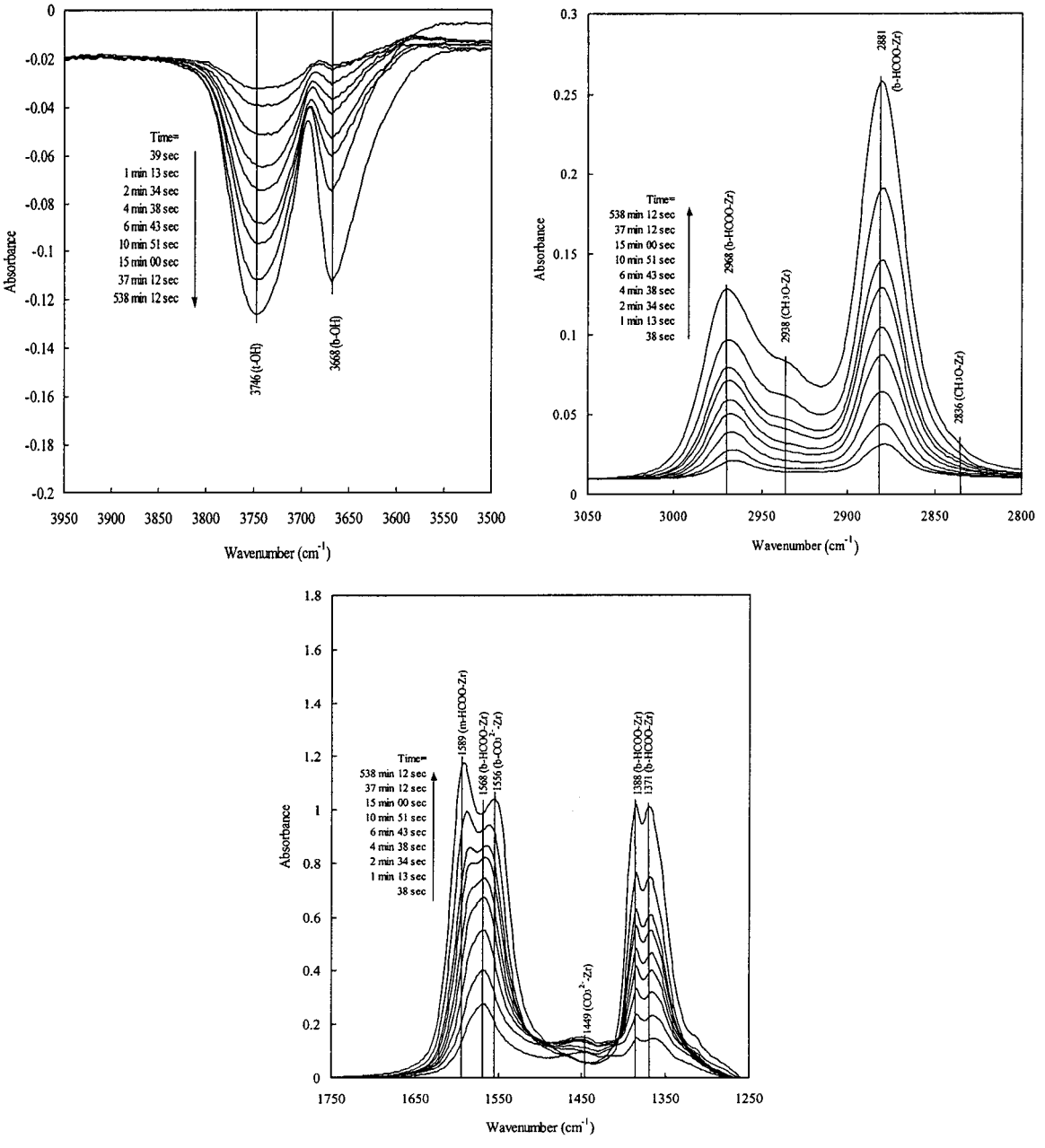

FIG. 8. Infrared spectra taken during exposure of ZrO_2 at 523 K to 488 kPa He and 162 kPa CO flowing at a total rate of 60 cm^3/min. Spectra are referenced to ZrO_2 under 650 kPa He flowing at 523 K.

b-HCOO–Zr species are formed by allowing CO to react with the hydroxl groups at 523 K and 654 kPa. The coverage of formate groups is $f = 0.30$ (f is the fraction of the maximum coverage) after 5 min of reaction and 0.8 after 20 min of reaction. After exposure, the catalyst is purged at 523 K and 101 kPa with 60 cm^3/min of He for 30 min to remove gaseous and adsorbed CO. The feed is then switched from He to D_2/He (1/3) at 423 K and a total pressure of 654 kPa. Half of the Zr–OH groups are changed to Zr–OD groups within 30 s of exposure to D_2 in the absence of formate species. In the presence of formate species this level of exchange occurs in 2 min when $f = 0.3$ and in 18 min when $f = 0.8$. As the formate coverage increases, the rate of H/D exchange of Zr–OH groups decreases and the exchange now occurs in two distinct stages.

To investigate the effect of formate presence on the exchange reaction of hydroxyls further, the effects of temperature and D_2 partial pressure are studied in the presence of formate. Formates are formed by reacting hydroxyls and CO at 523 K and 650 kPa for 20 min to maximize the surface

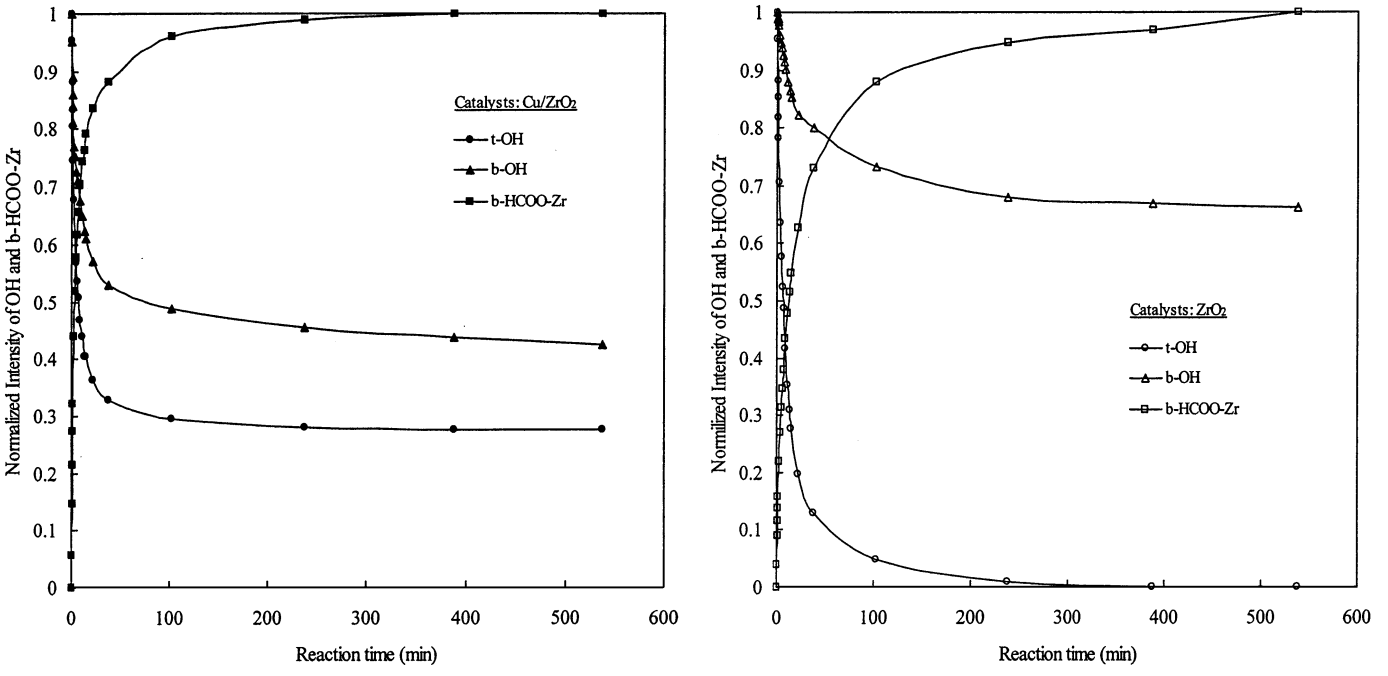

FIG. 9. Intensities of b-HCOO–Zr, t-OH, and b-OH features for both Cu/ZrO_2 and ZrO_2 from Figs. 6 and 7.

concentration b-HCOO–Zr while minimizing the formation of CH_3O–Zr. Before the H/D exchange was initiated, the catalyst was purged for 30 min with He of 60 cm^3/min at 523 K and 101 kPa.

Figure 11 shows plots of normalized OD band intensities as functions of time for temperatures of 398, 423, and 448 K and D_2 partal pressure of 488 kPa. Data for both Cu/ZrO_2 and ZrO_2 are shown. Similarly to the situation in

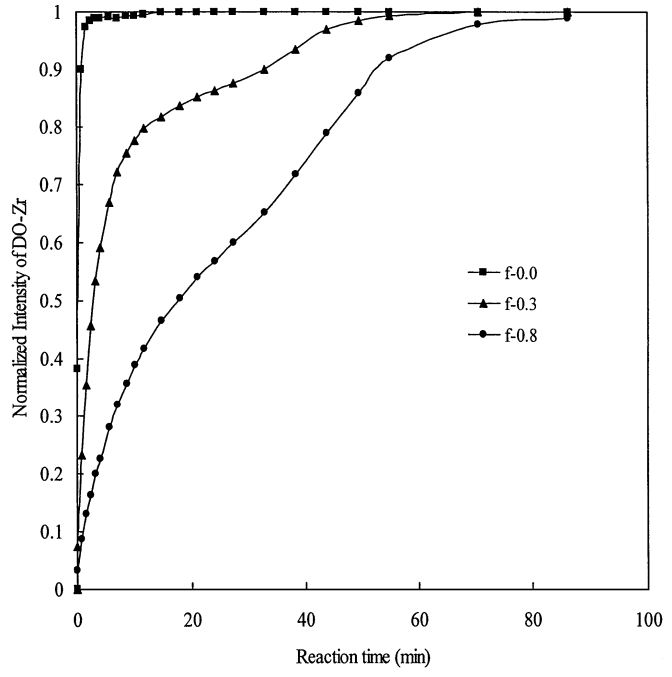

FIG. 10. Effects of formate groups ($f = 0.0$, 0.3, and 0.8) on the intensity of the DO–Zr band during exposure of Cu/ZrO_2 at 423 K to 488 kPa D_2 and 162 kPa He flowing at a total rate of 60 ml/min. Intensities are normalized to OD after total OH are changed to OD.

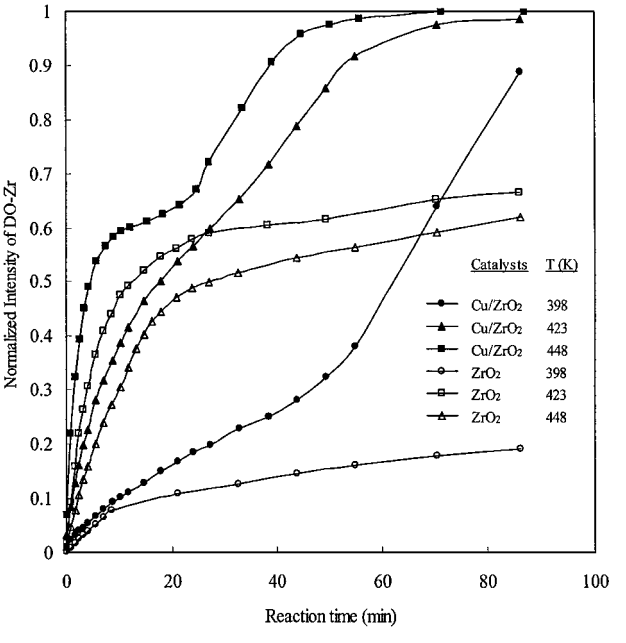

FIG. 11. Effects of formate groups ($f = 0.8$) on the intensity of the DO–Zr band during exposure of both Cu/ZrO_2 and ZrO_2 at 398 K, 423 K, and 448 K to 488 kPa D_2 and 162 kPa He flowing at a total rate of 60 cm^3/min. Intensities are normalized to that for DO–Zr after complete H/D exchange.

Fig. 10, the exchange of hydroxyls proceeds in two steps on Cu/ZrO_2. For ZrO_2 the first step is again visible but the second is much less pronounced than in the case of Cu/ZrO_2. Comparison of Figs. 5 and 11 reveals that the ratio of initial H/D exchange rates for hydroxyl groups without formate to initial rate with formate is 107 at 398 K for Cu/ZrO_2 and 2.5 for ZrO_2. These results indicate that the inhibiting effect of formate on the exchange reaction is more severe on Cu/ZrO_2 than on ZrO_2.

The apparent activation energies for H/D exchange of hydroxyl groups are presented in Table 1. The apparent activation energies are 72 kJ/mol on Cu/ZrO_2 and 66 kJ/mol on ZrO_2. These values are about 20% higher than those found in the absence of formate species (see Table 1). Table 1 also lists the dependence on D_2 partial pressure of the rate of H/D exchange observed in the presence of formate groups ($f = 0.8$). The order is 0.54 for Cu/ZrO_2 and 1.24 for ZrO_2.

H/D Exchange of Formate Groups

During the exchange reaction of hydroxyls in the presence of formate, HCOO–Zr can also undergo isotopic exchange. Figure 12 shows the spectra obtained during the isotopic exchange reaction on Cu/ZrO_2 at 423 K. Peaks are observable at 2968–2974 and 2876–2888 cm^{-1} for b-HCOO–Zr, at 2172–2181 cm^{-1} for b-DCOO–Zr, and at 2054–2062 cm^{-1} for CD_3O–Zr (20, 34). A band for C–H stretching vibrations of CHD_2O–Zr can be observed at 2888 cm^{-1} (20), but it overlaps a similar band associated with b-HCOO–Zr. During the exchange reaction, the peaks at 2888 and 2974 cm^{-1} shifted to 2875 and 2876 cm^1. Similarly, the peak at 2181 cm^{-1} for b-DCOO–Zr shifted to 2172 cm^{-1}, and the peak at 2062 cm^{-1} for CD_3O/CHD_2O–Zr shifted to 2054 cm^{-1}. The intensity of the peak at 2888 cm^{-1} for HCOO–Zr increases as the peak position shifts, while the intensity of the peak at 2974 cm^{-1} decreases monotonically. The intensiy of the peak at 2888 cm^{-1} for b-HCOO–Zr should not decrease, since b-HCOO–Zr is converted to b-DCOO–Zr and CD_3O/CHD_2O–Zr. The observed increase suggests that the extinction coefficient for b-HCOO–Zr increases as the peak shifts to lower frequency.

Figure 13 shows the spectra obtained during H/D exchange on ZrO_2 carried out at 423 K and in the presence of adsorbed formate species ($f = 0.8$). Peaks are observed at 2881 and 2970 cm^{-1} for b-HCOO–Zr and at 2176–2172 cm^{-1} for b-DCOO–Zr. Features were not observed for CD_3O/CHD_2O–Zr. As in the case of Cu/ZrO_2, the peak at 2881 cm^{-1} for b-HCOO–Zr shifted to 2873 cm^{-1} during the course of isotope exchange.

Figure 14 shows the normalized intensities of b-DCOO–Zr and CD_3O/CHD_2O–Zr on Cu/ZrO_2 and ZrO_2 calculated on the basis of the spectra presented in Figs. 12 and 13. The peak intensities are normalized to the intensity of b-HCOO–Zr before the exchange reaction. For Cu/ZrO_2 the transients for both b-DCOO–Zr and CD_3O–Zr exhibit two branches, similar to what was observed for the corresponding transient in HO–Zr seen in Fig. 11. It is also

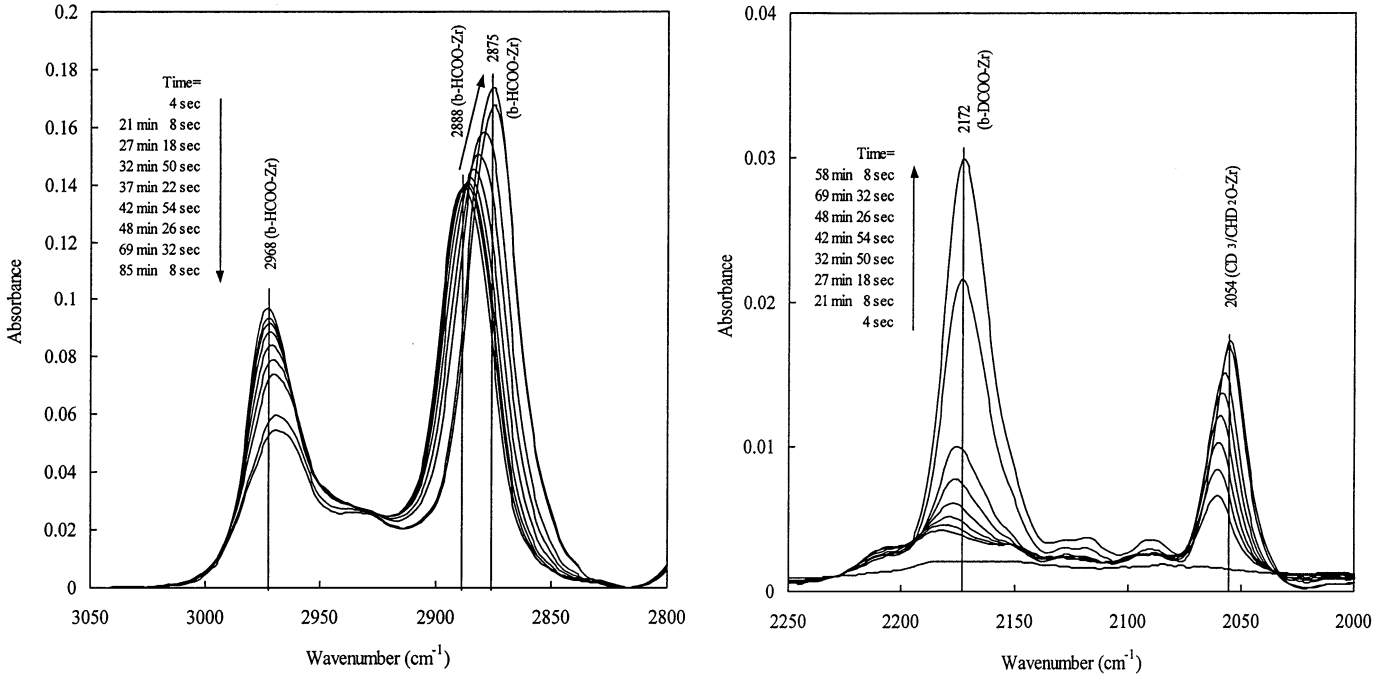

FIG. 12. Infrared spectra taken during exposure of Cu/ZrO_2 in the presence of formate species ($f = 0.8$) at 423 K to 488 kPa D_2 and 162 kPa He flowing at a total rate of 60 cm^3/min. Spectra are referenced to Cu/ZrO_2 purged in flowing He at 650 kPa and 423 K.

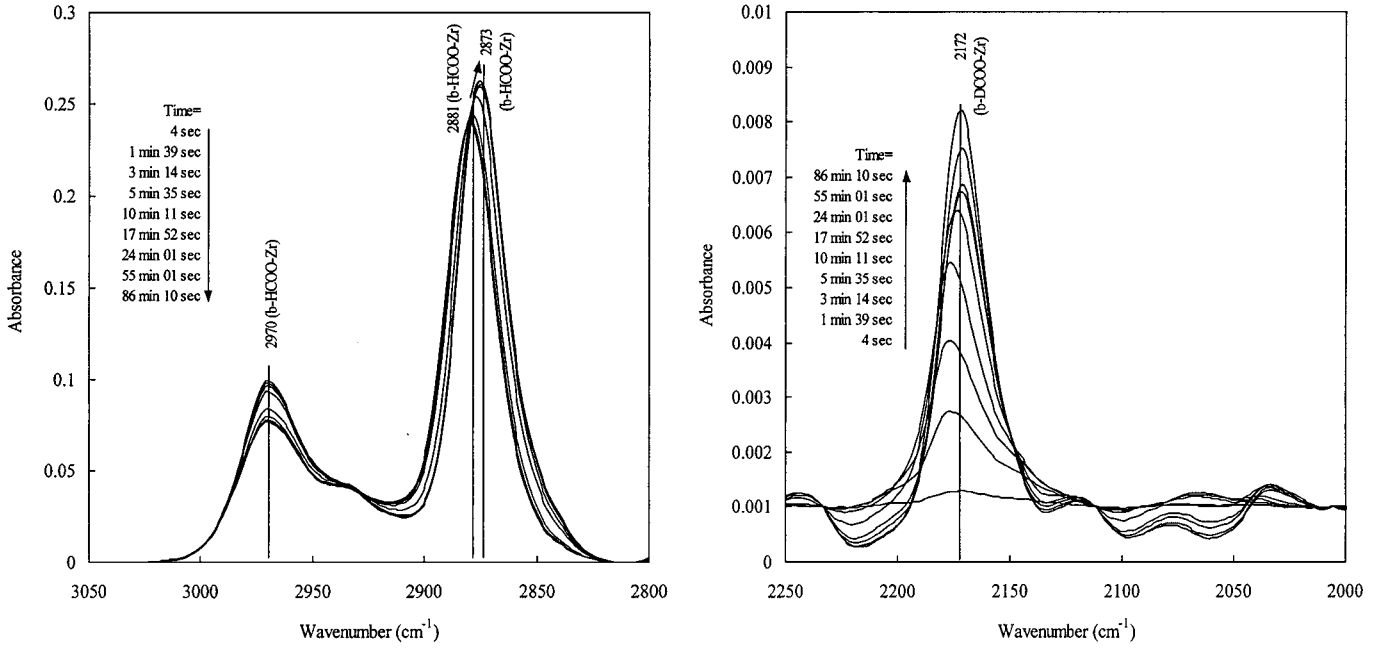

FIG. 13. Infrared spectra taken during exposure of ZrO_2 in the presence of formate species ($f = 0.8$) at 423 K to 488 kPa D_2 and 162 kPa He flowing at a total rate of 60 m1/min. Spectra are referenced to ZrO_2 purged in flowing He at 650 kPa and 423 K.

observed that the initial rate of H/D exchange is faster for formate than for methoxy groups. The transient for b-DCOO–Zr for ZrO_2 also resembles the corresponding transient in HO–Zr seen in Fig. 11. In this case, the first branch of the transient is clearly evident but not the second.

Figure 15 compares the change in the position of the b-HCOO–Zr band with the change in the normalized

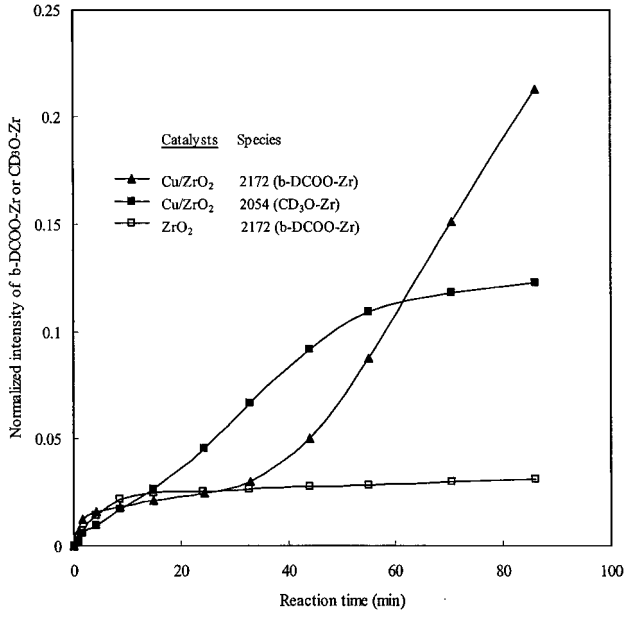

FIG. 14. Intensities of b-DCOO–Zr and CD_3O/CHD_2O–Zr bands during exposure of Cu/ZrO_2 and ZrO_2 in the presence of formate species ($f = 0.8$) at 423 K to 488 kPa D_2 and 162 kPa He flowing at a total rate of 60 cm^3/min. Intensities of b-DCOO–Zr and CHD_2/CD_3O–Zr are normalized to the intensity of the b-HCOO–Zr band observed at the beginning of the transient.

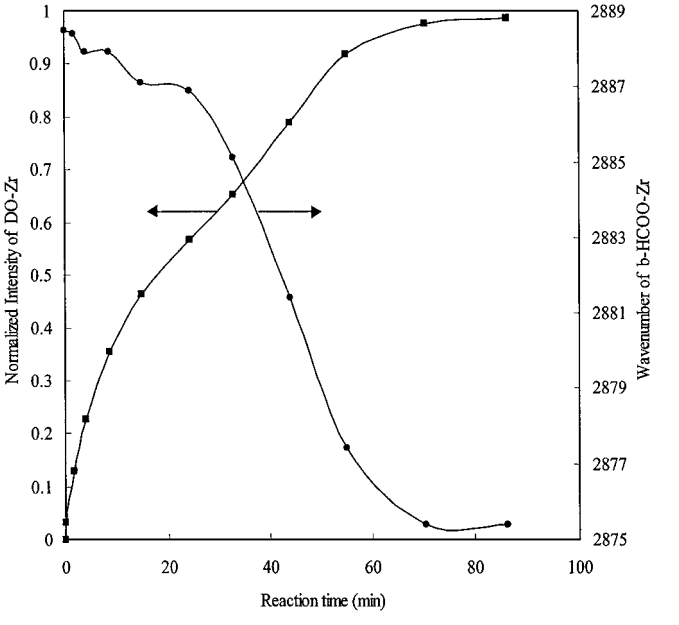

FIG. 15. Relationship between the intensity of the HO–Zr band and the position of the b-HCOO–Zr band obtained during exposure of Cu/ZrO_2 in the presence of formate species ($f = 0.8$) at 423 K to 488 kPa D_2 and 162 kPa He flowing at a total rate of 60 cm^3/min. The intensity of the DO–Zr band is normalized to that observed after complete H/D exchange.

intensity of the band for DO–Zr during the course of H/D exchange at 423 K. It is seen that the two functions plotted on the ordinate are correlated. As discussed below, the accelerated changes in both the position of b-HCOO–Zr and the intensity of the DO–Zr band, occurring during the period of 20–40 min into the H/D reaction, can be attributed to the formation of water via the process b-HCOO–Zr + 2 $D_2 \rightarrow CD_3O$–Zr + HDO. The adsorbed water formed via the hydrogenation of formate species leads to hydrogen bonding with the adsorbed formate species, and this, in turn, results in a downscale shift in the frequency of the b-HCOO–Zr band position (35). As was shown above, adsorbed water also accelerates the rate of H/D exchange of surface hydroxyl groups, and as will be shown below, adsorbed water accelerates the rate of H/D exchange of formate groups.

Effects of Water on H/D Exchange of Hydroxyl and Formate Species

To investigate the effects of adsorbed water on the dynamics of H/D exchange in the presence of formate groups, the H_2-reduced catalyst is first exposed to a CO/He mixture (1/3) at 523 K and 650 kPa for 20 min. The catalyst is then purged with He, cooled to 323 K, and exposed to 3.3 kPa of H_2O in flowing He. Finally, after another purge with He, the temperature is raised to 423 K and D_2 is introduced over the catalyst. Figure 16 shows plots of the normalized intensity of the DO–Zr band as a function of time. The presence of adsorbed water has opposite effects on the rates of exchange for Cu/ZrO_2 and ZrO_2. In the former case, adsorbed water strongly accelerates the rate of H/D exchange, but in the latter case the rate of H/D exchange in strongly retarded. These effects are similar to those observed in the absence of formate species (see Fig. 6).

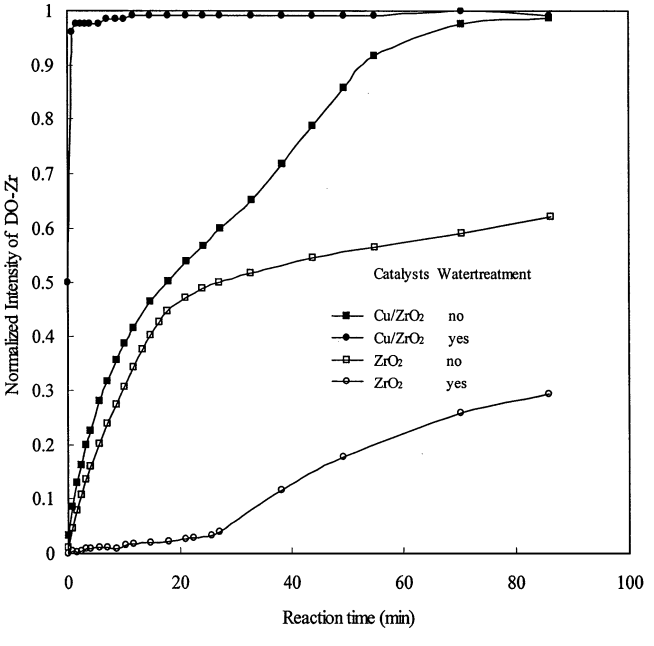

FIG. 16. Intensity of the DO–Zr band during exposure of Cu/ZrO_2 and ZrO_2 in the presence of formate ($f = 0.8$) at 423 K to 488 kPa D_2 and 162 kPa He flowing at a total rate of 60 cm^3/min. Prior to formate formation the samples were treated in water at 323 K (see text). The intensity of the DO–Zr band is normalized to that observed after complete H/D exchange.

Figure 17 shows spectra obtained at 423 K during the H/D exchange reaction on Cu/ZrO_2 pre-exposed to water vapor. When the surface is pretreated in water vapor, the peaks for b-HCOO–Zr occur at 2969 and 2875 cm^{-1} and do not shift over the course of exchange, as was seen in the absence of water vapor pretreatment (see Fig. 12). The reason for the absence of any shift in band position is that all formate groups experience hydrogen bonding from the outset of the exchange reaction. Similar effects of water vapor were also observed for H/D exchange occuring over ZrO_2 containing adsorbed formate species.

Figure 18 shows the effects of water vapor on the normalized intensity of b-DCOO–Zr and CD_3O/CHD_2O–Zr bands at 423 K during the isotope exchange on Cu/ZrO_2. Water vapor suppresses the formation of CD_3O/CHD_2O–Zr relative to what is observed in the absence of water vaopr, but significantly enhances the rate of H/D exchange with b-HCOO–Zr (see Fig. 14). This suggests that adsorbed water inhibits the hydrogenation of formate species to methoxy species, but adsorbed water through hydrogen bonding accelerates the rate of H/D exchange with formate species.

Formate Migration

Experiments were undertaken to study the migration of formate species from Cu to ZrO_2. Since evidence of formate species associated with Cu cannot be observed for Cu/ZrO_2 catalysts or Cu/SiO_2 catalysts heavily promoted with ZrO_2 (17), these experiments were carried out with a $Cu/ZrO_2/SiO_2$ catalyst in which the components are present in the weight ratio of 5/15/80. The catalyst was exposed to CO_2/H_2 (1/3) at a total pressure of 650 kPa. As seen in Fig. 19, features are observable at 2938, 2856, and 1352 cm^{-1} for b-HCOO–Cu and at 2981 and 1364 cm^{-1} for m-HCOO–Cu. Peaks for b-HCOO–Zr are observed at 2972, 2893, 1586, 1388, and 1373 cm^{-1} for b-HCOO–Zr, at 1624 cm^{-1} for b-HCO_3–Zr, and at 1448 cm^{-1} for i-CO_3–Zr. The peak at 2952 cm^{-1} can be assigned to H_2CO_2–Zr (16, 17). These spectra demonstrate that the formate groups associated with Cu and ZrO_2 can readily be differentiated.

After reaction has occurred for 90 min, the catalyst is exposed to He flowing at 60 cm^3/min for 40 min. Reaction for 90 min followed by purge for 40 min is then repeated. Figure 20 shows the spectra obtained during the reaction and He purge cycle at 373 K and 650 kPa. During He purge after the reaction, the peaks for b-HCOO–Cu

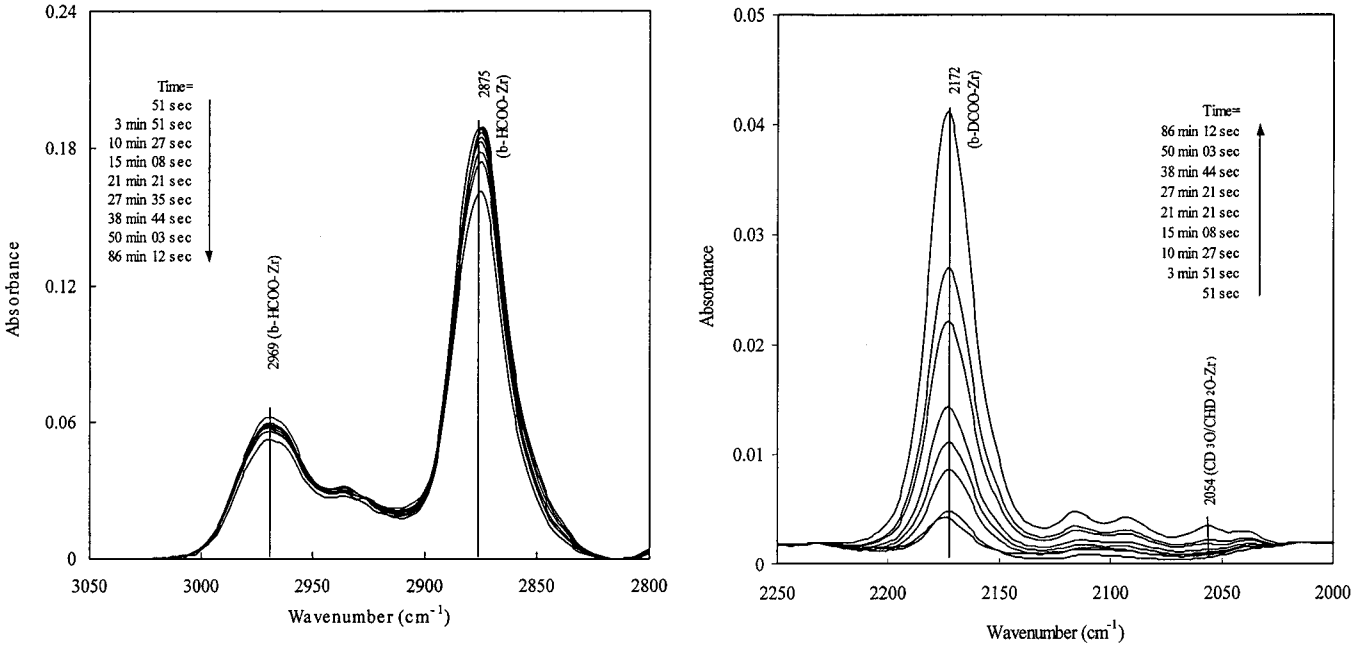

FIG. 17. Infrared spectra taken during exposure of Cu/ZrO_2 in the presence of formate ($f = 0.8$) at 423 K to 488 kPa D_2 and 162 kPa He flowing at a total rate of 60 cm^3/min. Samples were treated with water vapor at 323 K prior to the initiation of H/D exchange (see text). Spectra are referenced to Cu/ZrO_2 purged under 650 kPa He flowing at 423 K.

decrease while the peaks for b-HCOO–Zr increase. Repeated cycling shows the same results. While it is possible that the decrease in the intensity of b-HCOO–Cu is due to decomposition into H_2 and CO_2, this process only starts to occur at 400–430 K (36–38). A more plausible interpretation is that formate species migrate form Cu to ZrO_2.

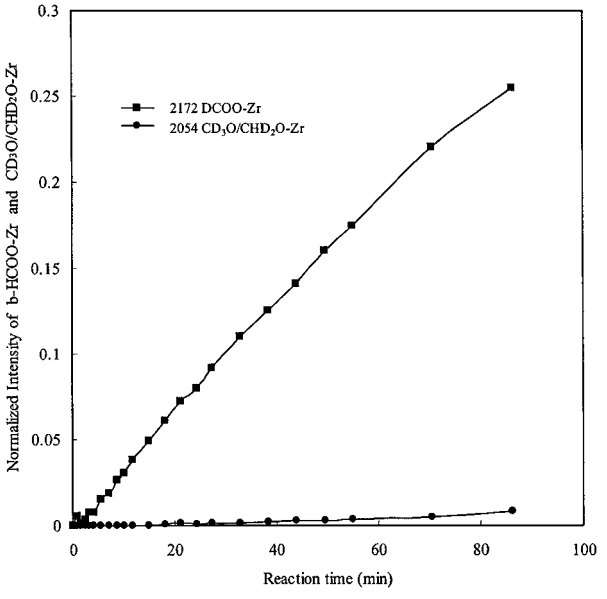

FIG. 18. Intensities of b-DCOO–Zr and CD_3O/CHD_2O–Zr bands during exposure of Cu/ZrO_2 and ZrO_2 in the presence of formate ($f = 0.8$) at 423 K to 488 kPa D_2 and 162 kPa He flowing at a total rate of 60 cm^3/min after water treatment. The intensities of the b-DCOO–Zr and CHD_2/CD_3O–Zr bands are normalized to that of the b-HCOO–Zr band observed at the beginning of the transient.

DISCUSSION

H/D Exchange of Zr–OH Groups in the Absence of Formate Species

In the absence of formate groups on the surface of zirconia, the rate at which Zr–OH groups undergo H/D exchange is strongly dependent on the presence of dispersed Cu (see Fig. 5). This observation is similar to that reported earlier for the effects of dispersed Rh on hydroxyl group H/D exchange on the surface of zirconia and other metal oxides (21). The strong enhancement in the rate of H/D exchange in the presence of the dispersed metal is attributed to an increase in the ease with which gas-phase H_2 or D_2 can be adsorbed dissociatively, since it is assumed that the availability of some form of atomically adsorbed H(D) is a prerequisite for isotopic exchange of the hydrogen atoms associated with the hydroxyl groups (39).

While dissociative adsorption of $H_2(D_2)$ is presumed by the authors of all previous studies of H/D exchange of hydroxyl groups on ZrO_2, the nature of the rate-limiting step is not clearly identified. For example, Domen and coworkers (19, 20) assume that isotopic exchange of hydroxyl groups on ZrO_2 is controlled by the intrinsic rate of the process $D^* + Zr–OH \rightarrow H^* + Zr–OD$, where H*(D*) is some form of mobile atomic hydrogen and Zr–OH(Zr–OD) is

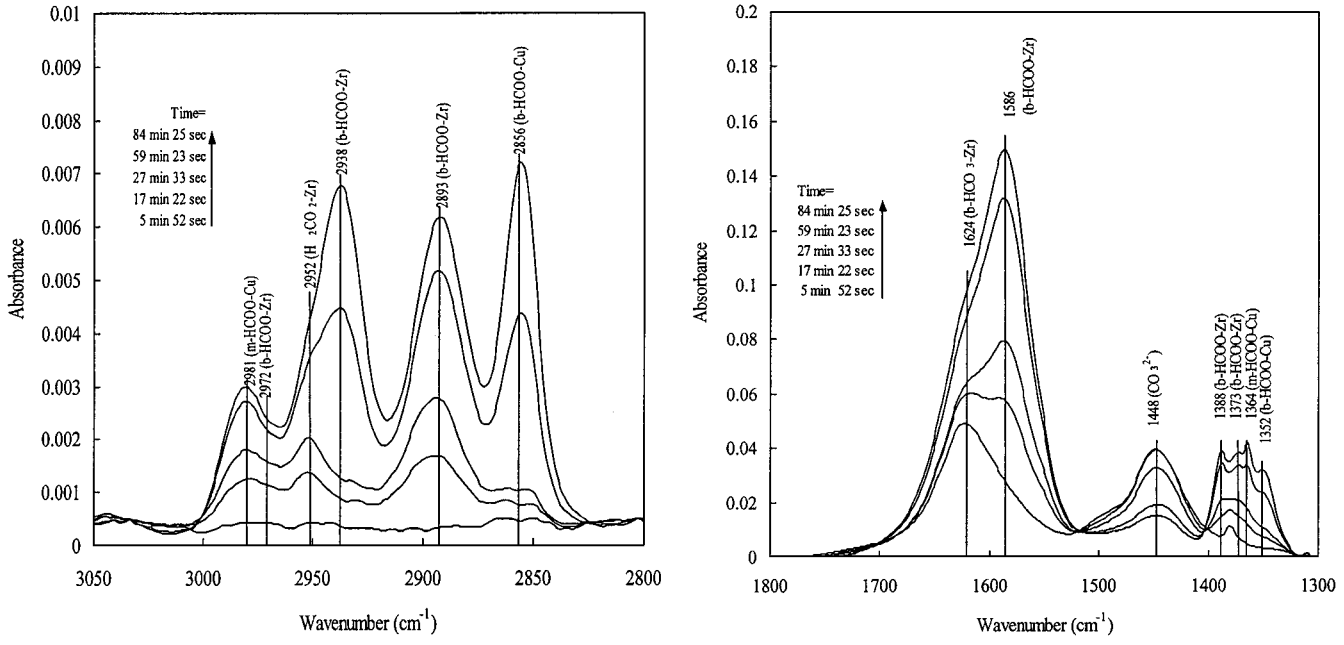

FIG. 19. Infrared spectra taken during exposure of $Cu/ZrO_2/SiO_2$ at 373 K to 488 kPa H_2 and 162 kPa CO_2 flowing at a total rate of 60 cm^3/min. Spectra are referenced to Cu/ZrO_2 reduced in 650 kPa H_2 flowing at 373 K.

a hydroxyl group on the surface of zirconia. In contrast, Martin and Duprez (21) assume that above 348 K, H/D exchange of hydroxyl groups on Rh/ZrO_2 is controlled by the diffusion of hydrogen (i.e., H*(D*)). Since neither set of authors provides any justification for their assumption, it is necessary to develop a criterion by which one might make a reasonable assessment of the controlling factors for a given set of circumstances.

The mechanisms by which H/D exchange of hydrogen in Zr–OH groups might occur in the presence and absence of Cu on the surface of ZrO_2 can be envisoned in the following manner. In the absence of Cu, $H_2(D_2)$ has been reported to

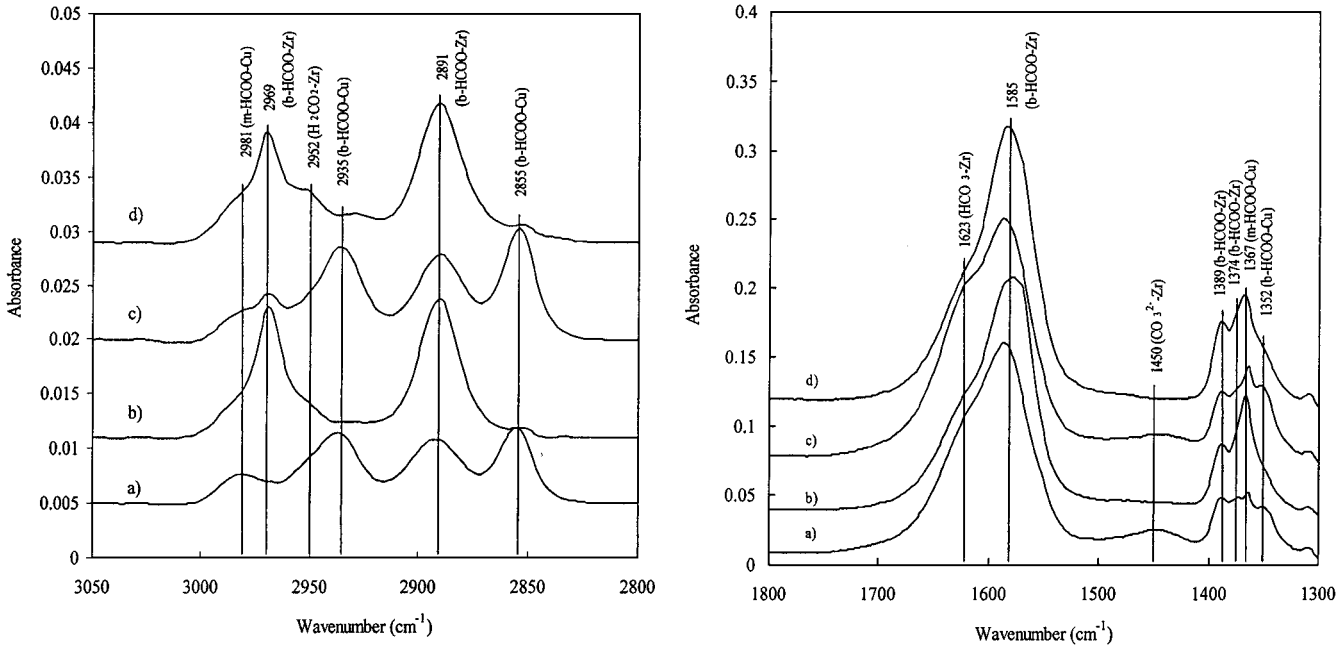

FIG. 20. Infrared spectra taken after exposure of $Cu/ZrO_2/SiO_2$ at 373 K to (a) 488 kPa H_2 and 162 kPa CO_2, (b) 650 kPa He, (c) 488 kPa H_2 and 162 kPa CO_2, again, and (d) 650 kPa He, again, flowing at a total rate of 60 cm^3/min. Spectra are referenced to Cu/ZrO_2 reduced in 650 kPa H_2 flowing at 373 K.

adsorb dissociatively either homolytically (40, 41) or heterolytically (41). The literature does not establish clearly which of these two processes predominates, and arguments have been made for each extreme (40–42). When Cu is dispersed on the surface of ZrO_2, dissociative adsorption of $H_2(D_2)$ is presumed to occur predominantly on the Cu surface. Previous studies have shown that the activation barrier for H_2 adsoption is ~34 kJ/mol and the heat of dissociative adsorption is ~46 kJ/mol on Cu (43). It seems reasonable to assume that the processes of dissociative adsorption and recombinative desorption are at equilibrium with respect to the gas partial pressure of $H_2(D_2)$ for the temperatures used in the present study. The species that diffuses across the surface of ZrO_2 and is ultimately involved in H/D exchange is designated H*(D*). While the bonding of such a species to metal oxides has been discussed, no definitive conclusion as to its charge or mode of bonding has been established (42). For the sake of this discussion, we assume that the surface concentration of H*(D*) in the immediate vicinity of the $H_2(D_2)$ dissociation centers is at equilibrium with the surface concentration of atomically adsorbed H(D). For a hydroxyl group to undergo H/D exchange, H*(D*) must diffuse across the surface of ZrO_2 and then react with an OH(OD) group. The issue then, is to ascertain whether surface diffusion is a rate-limiting step. A useful criterion for this purpose is that developed by Weisz and Prater (44) to determine whether intraparticle mass transfer affects the overall rate of reaction occurring within a catalyst particle. The Weisz–Prater analysis requires that the dimensionless parameter Φ_s be less than unity, where Φ_s is defined as follows,

$$\Phi_s = \frac{r_{ex} R^2}{C^o_{D^*} D_s}, \qquad [1]$$

where r_{ex} is the experimentally observed rate of H/D exchange, R is one-half of the average distance between $H_2(D_2)$ dissociation centers, $C^o_{D^*}$ is the maximum surface concentration of H*(D*), and D_s is the surface diffusion coefficient for H*(D*).

To determine whether the Weisz–Prater criterion is satisfied, we consider first the conditions under which the fastest rate of exchange occurs. This corresponds to exchange occurring in the presence of Cu at 398 K. The apparent first-order rate coefficient for this case determined on the basis of the data shown in Fig. 5 is 4×10^{-2} s^{-1}. If we take the concentration of OH groups on the surface of ZrO_2 to be 10^{14} molecules/cm^2 (21), then the maximum rate of exchange at $t = 0$ is 4×10^{12} molecules/cm^2 s. The average distance between Cu crystallites is estimated to be 10^{-4} cm on the basis of the Cu loading and dispersion; therefore, $R = 5 \times 10^{-5}$ cm. Neither the surface concentration nor the diffusion coefficient for H*(D*) is known; hence, the magnitudes of these quantities can only be estimated. Previous studies suggest that D_s will lie within the broad range of 10^{-15} cm^2/s to 10^{-4} cm^2/s (21, 39). The lower bound seems unrealistically low, and may be a consequence of the authors' assumption that the observed rate of H/D exchange on the surface of Rh/ZrO_2 is controlled by surface diffusion. If the results of this particular work are excluded, then the range of values for D_s narrows to 10^{-10}–10^{-4} cm^2/s. Taking this range of values for D_s leads to the conclusion that $C^o_{D^*}$ must be greater than 10^8 atoms/cm^2 for rate of isotopic exchange to be unaffected by diffusional transport across the surface of ZrO_2. While it cannot be proven, it is suspected that the surface concentrations of H*(D*) are more than adequate for the Weisz–Prater criterion to be satisfied. If this is true, then virtually all of the observed rates of H/D exchange reported here are governed by the intrinsic rate of the process $D^* + Zr\text{–}OH \rightarrow H^* + Zr\text{–}OD$. Indirect support for this conclusion is provided by the observation that the activation barriers for H/D exchange obtained in the absence and in the presence of Cu are essentially the same (see Table 1). If the nearly thousand-fold faster rate of H/D exchange observed in the presence of Cu were influenced significantly by surface diffusion but the rate of H/D exchange over ZrO_2 in the absence of Cu were controlled by the rate of the intrinsic kinetics, then one would anticipate different values for the apparent activation energies. Some evidence for the influence of diffusional limitations on the rate of isotopic transport will be noted below when the effects of water vapor are discussed.

The higher rate of H/D exchange of hydroxyl groups on ZrO_2 observed when dispersed Cu is present is attributed to a higher surface concentration of H*(D*). If, as was assumed earlier, gas-phase $H_2(D_2)$ is in equilibrium with the dissociative adsorption centers present on the surface of ZrO_2 or Cu and the maximum surface concentration of H*(D*) is in equilibrium with the surface concentration of dissociatively adsorbed $H_2(D_2)$, then one might expect the dependence of the surface concentration of H*(D*), C_{H^*}, to take the form

$$C_{H^*} = \frac{A p_{H_2}^{1/2}}{\left(1 + B p_{H_2}^{1/2}\right)},$$

where p_{H_2} is the partial pressure of H_2 and A and B are constants. Consistent with this model, the partial pressure dependence should lie between 0.5 and 0. Table 1 shows that the observed values of the partial pressure dependence are 0.25 in the absence of formate species and 0.54 in the presence of formate species, which is in agreement with the proposed model of H_2 activation and spillover.

As noted earlier, water adsorbed on the surface of ZrO_2 has completely opposite effects on the rate of H/D exchange of hydroxyl groups present on the surface of Cu/ZrO_2 and ZrO_2. The significant retardation in the isotopic exchange rate observed in the absence of Cu (see Fig. 6) can be attributed to the suppression of $H_2(D_2)$ dissociative adsorption. IR and EPR studies show that both water and carbon

dioxide inhibit the dissociative adsorption of H_2 on Zr^{3+} centers (45). By contrast, H_2O does not adsorb strongly on the surface of Cu and, hence, does not affect the dissociative adsorption of $H_2(D_2)$. Figure 6 shows that the presence of water vapor slightly enhances the rate of H/D exchange in the case of Cu/ZrO_2. This can be attributed to an enhancement in the rate of H*(D*) migration across the ZrO_2 surface via hydrogen-bonded water bridges. These structures enable the facile transfer of isotopically labeled hydrogen as a consequence of the exchange of hydrogen atoms between water molecules, a mechanism similar to that suggested previously for the role of water in enhancing H/D exchange in zeolites (46). The observation of a small increase in the rate of H/D exchange when Cu is dispersed on the ZrO_2 surface suggests that the rate of isotopic exchange in the absence of water is on the borderline of being influenced by diffusional transport.

H/D Exchange of Zr–OH Groups in the Presence of Formate Groups

During the hydrogenation of CO_2 to methanol the most abundant surface species are formate groups adsorbed on ZrO_2 (17). As was shown in Figs. 10 and 11 these groups inhibit H/D exchange of Zr–OH groups. The initial rates at which hydroxyl groups undergo H/D exchange are comparable for ZrO_2 and Cu/ZrO_2; however, in the case of Cu/ZrO_2 the rate of H/D exchange undergoes an acceleration after a period of time. The onset of accelerated H/D exchange comes at a progressively earlier time as the temperature at which exchange begins increases. During the period of accelerated H/D exchange the position of the formate bands shift to slightly lower frequencies (see Figs. 13 and 14). As was observed in the absence of formate species, the presence of water vapor on the surface of ZrO_2 retards the rate at which Zr–OH groups undergo H/D exchange over ZrO_2, but has the opposite effect on the rate of isotopic exchange over Cu/ZrO_2. Moreover, the period of accelerated exchange is completely eliminated. When water vapor is present the frequencies of the formate bands are identical to those observed during the accelerated H/D exchange over Cu/ZrO_2.

It is proposed that the presence of formate groups on the surface of ZrO_2 decreases the number of sites where $H_2(D_2)$ can dissociate as well as partially blocking (frustrating) the path for H*(D*) transport. Both effects reduce the rate of H/D exchange on ZrO_2. When Cu is present, only the second of these effects is relevant, since $H_2(D_2)$ dissociation occurs primarily on Cu. It is surprising though that the inhibition of H/D exchange of hydroxyl groups is significantly greater for Cu/ZrO_2 than for ZrO_2 (see above). This may imply that surface transport limitations play a more important role in the former case than in the latter. The beneficial effects of water are again due to the formation of hydrogen-boded chains of water molecules on the surface of ZrO_2.

Comparison of the Dynamics of H/D Exchange with the Dynamics of Methanol Synthesis

As noted in the Introduction, previous studies of methanol synthesis over $Cu/ZrO_2/SiO_2$ and Cu/ZrO_2 have demonstrated that Cu and ZrO_2 play separate functions during the synthesis of methanol from either CO/H_2 or CO_2/H_2 (16, 17). CO or CO_2 is adsorbed on the surface of ZrO_2 via reaction with Zr–OH groups to form formate or bicarbonate species, which then undergo subsequent hydrogenation to produce methanol. The hydrogen required for the latter process is supplied by dissociative adsorption of H_2 on Cu followed by spillover of atomic H onto ZrO_2. The results of the present investigation support this view. Examination of the spectra shown in Fig. 9 shows that the adsorption of CO results in the loss of OH groups and the concurrent appearance of HCOO–Zr groups. The pseudo-first-order rate coefficients for this process are $1.8 \times 10^{-5}\,s^{-1}$ and $3.5 \times 10^{-5}\,s^{-1}$ for ZrO_2 and Cu/ZrO_2, respectively. The somewhat higher value of the rate coefficient for Cu/ZrO_2 may be due to the higher rate of CO accumulation on the surface of ZrO_2 as a consequence of CO spillover from the surface of Cu (18). However, for both catalysts HCOO–Zr groups are formed primarily via the process $CO_{(g)} + Zr–OH \rightarrow HCOO–Zr$. Since previous work (18) has shown that the rate of formate formation on the surface of Cu is much slower than the rate at which these species are formed on the surface of ZrO_2, the possibility of formate spillover to ZrO_2 can be excluded as a signficant contributor to the dynamics of formate formation on Cu/ZrO_2.

By contrast, the dynamics of formate formation from CO_2/H_2 is much faster on Cu/ZrO_2 than on ZrO_2, as can be seen by examination of Fig. 3. This can be attributed to the following factors. The adsorption of CO_2 on ZrO_2 produces HCO_3–Zr species that are converted to HCOO–Zr by hydrogenation (17). In the absence of an adequate supply of atomic hydrogen on the surface of ZrO_2, this process is slow. As discussed above, the presence of dispersed Cu ensures the supply of atomic hydrogen via the process of spillover. Yet another process may also contribute to the accelerated formation of formate species on the surface of ZrO_2 when Cu is present. The experiments presented in Fig. 20 demonstrate that formate species can form on the surface of Cu via direct hydrogenation of adsorbed CO_2 and that such formate groups can spill over onto the ZrO_2. While the dynamics of this latter process have not been established quantitatively, it is felt that the spillover of formate species from Cu to ZrO_2 is not an important contributor to the overall dynamics of formate species formation on ZrO_2.

Having established the role of hydrogen spillover on the synthesis of methanol over Cu/ZrO_2, it is important to assess whether the rate of spillover is rapid or slow relative to the rate of formation of methanol and intermediates leading to the formation of methanol. The pseudo-first-order rate

coefficient for H/D exchange of Zr–OH groups will be used as a measure of the lower bound on the rate of hydrogen spillover. The reason that this rate represents a lower bound is that in the absence of diffusional mass transfer limitation, the rate of H/D exchange of Zr–OH groups is dictated by the rate of the process $D^* + Zr\text{–}OH \rightarrow H^* + Zr\text{–}OD$. However, the rate of spillover can be faster than this rate. Since previous studies have shown that the rate of methanol synthesis from both CO and CO_2 parallels the rate of appearance of CH_3O–Zr species on the surface of ZrO_2, the pseudo-first-order rate coefficient for the formation of CH_3O–Zr can be used as a measure of the rate of methanol synthesis (17, 18).

At 523 K and under the conditions shown in Fig. 3, the pseudo-first-order rate coefficient for the formation of CH_3O–Zr is $7 \times 10^{-2}\ s^{-1}$. The pseudo-first-order rate coefficient for H/D exchange of HO–Zr groups in the presence of formate groups is estimated from Fig. 16 as $8 \times 10^{-4}\ s^{-1}$ for 373 K. Assuming an activation energy of 17.2 kcal/mol (see Table 1) leads to an estimate of $6 \times 10^{-1}\ s^{-1}$ at 523 K for this pseudo-first-order rate coefficient. This means that the rate of hydrogen spillover is at least an order of magnitude faster than the rate of methanol synthesis and thus will not constitute a rate-limiting step under the conditions of the experiments reported here. It is important to note that the rate of hydrogen spillover from the supported Cu crystallites is expected to scale with the Cu loading and dispersion. In fact, the product of these two quantities is proportional to the Cu surface area. Thus, it would appear that the rate of methanol synthesis might not be affected by a reduction in the amount of exposed Cu surface relative to that used in the present studies. Such a change should to lead to an improvement in the methanol selectivity for synthesis from CO_2/H_2 mixtures, since it has been shown that the reverse water–gas shift reaction ($CO_2 + H_2 \rightarrow CO + H_2O$) occurs on the surface of Cu but not on ZrO_2 (17).

CONCLUSIONS

The dynamics of H/D exchange on the surface of ZrO_2 are found to depend on a number of factors including the presence of dispersed Cu, the $H_2(D_2)$ partial pressure, the temperature, and the presence of adsorbed water. The rate of H/D exchange of HO–Zr groups is much more rapid in the presence than in the absence of Cu dispersed on the surface of ZrO_2. This effect is attributed to the higher effectiveness of Cu to dissociate $H_2(D_2)$. The rate of H/D exchange increases with temperature and the apparent activation energies for ZrO_2 and Cu/ZrO_2 are 50 kJ/mol and 53 kJ/mol, respectively. Consistent with the similarity in the activation energies and with an estimate of the degree of mass transfer limitation on the exchange process, it is concluded that the rate of H/D exchange is controlled by the process $D^* + HO\text{–}Zr - H^* + DO\text{–}Zr$. The apparent partial pressure dependence on $H_2(D_2)$ is 0.74 for ZrO_2 and 0.25 for Cu/ZrO_2, which reflects the differences in the types of sites involved in the dissociative activation of $H_2(D_2)$ on the two types of catalyst. While adsorbed water significantly inhibits the rate of H/D exchange on ZrO_2, the opposite effect is observed for Cu/ZrO_2. The reason is that adsorbed water inhibits the dissociation of $H_2(D_2)$ on the surface of ZrO_2 but not on the surface of Cu. Adsorbed water facilitates the transport of H(D) atoms formed on the surface of Cu across the surface of ZrO_2 as a consequence of hydrogen bonding between adsorbed H_2O and HO–Zr groups. Formate groups are formed on the surface of ZrO_2 primarily via the process $CO_{(g)} + HO\text{–}Zr \rightarrow HCOO\text{–}Zr$. Such groups can also form on the surface of Cu and spill over onto the surface of ZrO_2. The presence of formate groups inhibits the rate of H/D exchange of HO–Zr groups. As in the absence of formate groups, adsorbed water inhibits the rate of H/D exchange for ZrO_2 but enhances it for Cu/ZrO_2. The dynamics of H/D exchange are compared with the dynamics of methanol formation as measured by the rate of CH_3O–Zr formation on Cu/ZrO_2. On the basis of this analysis it is concluded that the rate of hydrogen spillover from Cu is more than an order of magnitude faster than the rate of methanol formation, and, hence, not a rate-limiting step in the synthesis of methanol over Cu/ZrO_2.

ACKNOWLEDGMENTS

This work was supported by the Director of the Office of Basic Energy Sciences, Chemical Sciences Division, of the U.S. Department of Energy under Contract DE-AC03-76SF00098.

REFERENCES

1. Denise, B., and Sneeden, R. P. A., *Appl. Catal.* **28**, 235 (1986).
2. Chen, H. W., White, J. M., and Ekerdt, J. G., *J. Catal.* **99**, 293 (1986).
3. Amenomiya, Y., *Appl. Catal.* **30**, 57 (1987).
4. Denise, B., Sneeden, R. P. A., Beguin, B., and Cherifi, E., *Appl. Catal.* **30**, 353 (1987).
5. Jackson, N. B., and Ekerdt, J. G., *J. Catal.* **101**, 90 (1986).
6. Koeppel, R. A., Baiker, A., Schild, C., and Wokaun, A., *in* "Preparation of Catalysts V" (G. Poncelet, P. A. Jacobs, P. Grange, and B. Delmon, Eds.), Stud. Surf. Sci. Catal. Vol. 63, p. 59. Elsevier, Amsterdam, 1991.
7. Kanoun, N., Astier, M. P., and Pajonk, G. M., *Catal. Lett.* **15**, 231 (1992).
8. Sun, Y., and Sermon, P. A., *J. Chem. Soc., Chem. Commun.* 1242 (1993).
9. Nitta, Y., Suwata, O., Ikeda, Y., Okamoto, Y., and Imanaka, T., *Catal. Lett.* **26**, 345 (1994).
10. Fisher, I. A., Woo, H. C., and Bell, A. T., *Catal. Lett.* **44**, 11 (1997).
11. Koppel, R. A., Stocker, C., and Baiker, A., *J. Catal.* **179**, 515 (1998).
12. Koeppel, R. A., Baiker, A., and Wokaun, A., *Appl. Catal.* **84**, 77 (1992).
13. Sun, Y., and Sermon, P. A., *Catal. Lett.* **29**, 361 (1994).
14. Schid, C., Wokaun, A., and Baiker, A., *J. Mol. Catal.* **63**, 243 (1990).
15. Weigel, J., Koeppel, R. A., Baiker, A., and Wokaun, A., *Langmuir* **12**, 5319 (1996).
16. Ortelli, E. E., Weigel, J. M., and Wokaun, A., *Catal. Lett.* **54**, 41 (1998).
17. Fisher, I. A., and Bell, A. T., *J. Catal.* **172**, 222 (1997).
18. Fisher, I. A., and Bell, A. T., *J. Catal.* **178**, 153 (1998).

19. Ouyang, F., Kondo, J. N., Maruya, K. I., and Domen, K., *J. Chem. Soc., Faraday Trans.* **92**, 4491 (1996).
20. Ouyang, F., Kondo, J. N., Maruya, K. I., and Domen, K., *J. Chem. Soc., Faraday Trans.* **93**, 169 (1997).
21. Martin, D., and Duprez, D., *J. Phys. Chem.* **101**, 4428 (1997).
22. Hicks, R. F., Kellner, C. S., Savatsky, B. J., Hecker, W. C., and Bell, A. T., *J. Catal.* **71**, 216 (1981).
23. Kondo, J., Abe, H., Sakata, Y., Maruya, K., Domen, K., and Onish, T., *J. Chem. Soc., Faraday Trans. 1* **84**, 511 (1998).
24. Bianchi, D., Chafik, T., Khalfallah, M., and Teichner, S. J., *Appl. Catal.* **123**, 89 (1993).
25. Bianchi, D., Chafik, T., Khalfallah, M., and Teichner, S. J., *Appl. Catal.* **105**, 223 (1993).
26. Hertl, W., *Langmuir* **5**, 96 (1989).
27. Guglieliminotti, E., *Langmuir* **6**, 1455 (1990).
28. Bensitel, M., Saur, O., and Lavalley, J., *Mater. Chem. Phys.* **17**, 249 (1987).
29. He, M.-Y., and Ekerdt, J. G., *J. Catal.* **87**, 381 (1984).
30. Clarke, D. B., Lee, D. K., Sandoval, M. J., and Bell, A. T., *J. Catal.* **150**, 81 (1994).
31. Millar, G. J., Rochester, C. H., Howe, C., and Waugh, K. C., *Mol. Phys.* **76**(4), 833 (1991).
32. Agron, P. A., Fuller, E. L., Jr., and Holmes, H. F., *J. Colloid Interface Sci.* **52**, 553 (1975).
33. Bianchi, D., Chafik, T., Khalfallah, M., and Teichner, S. J., *Appl. Catal.* **112**, 219 (1994).
34. Bensitel, M., Morawek, V., Lamotte, J., Saur, O., and Lavalley, J. C., *Spectrochim. Acta Part A* **43**, 1487 (1987).
35. Bianchi, D., Chafik, T., Khalfallah, M., and Teichner, S. J., *Appl. Catal.* **101**, 297 (1993).
36. Ying, D., and Madix, R. J., *J. Catal.* **61**, 48 (1980).
37. Poulston, S., Rowbotham, E., Stone, P., Parlett, P., and Bowker, M., *Catal. Lett.* **52**, 63 (1998).
38. Clark, D. B., and Bell, A. T., *J. Catal.* **154**, 314 (1995).
39. Conner, W. C., Jr., and Flaconer, J. L., *Chem. Rev.* **95**, 759 (1995).
40. Jacob, K., Knozinger, E., and Benter, S., *J. Chem. Soc., Faraday Trans.* **90**, 2969 (1994).
41. Kondo, J., Sakata, Y., Domen, K., Maruya, K., and Onishi, T., *J. Chem. Soc., Faraday Trans.* **86**, 397 (1990).
42. Roland, U., Brauschwieg, T., and Roesner, F., *J. Mol. Catal.* **127**, 64 (1997).
43. Sandoval, M. J., and Bell, A. T., *J. Catal.* **144**, 227 (1993).
44. Fogler, H. S., "Elements of Chemical Reaction Engineering", 2nd ed. Prentice Hall, New York, 1992.
45. Morterra, L., Giamello, E., Orio, L., and Volante, M., *J. Phys. Chem.* **94**, 3111 (1990).
46. Dalla Betta, R. A., and Boudart, M., *J. Chem. Soc., Faraday Trans. 1* **72**, 1723 (1976).